Supplementary information

PbI_2 Heterogeneous-Cap-Induced Crystallization for Efficient $CH_3NH_3PbI_3$ Layer in Perovskite Solar Cells

Yangrunqian Wang,[ab] Jiawei Li,[ab] Qian Li,[ab] Weidong Zhu,[ab] Tao Yu,[*abcd] Xingyu Chen,[ab] Lu'an Yin,[a] Yong Zhou,[abcd] Xiaoyong Wang,[a] Zhigang Zou[abcd]

[a.] National Laboratory of Solid State Microstructures, Nanjing University, Nanjing 210093, P. R. China.

E-mail: yutao@nju.edu.cn

[b.] Ecomaterials and Renewable Energy Research Center (ERERC) at Department of Physics, Nanjing University, Nanjing 210093, P. R. China

[c.] Collaborative Innovation Center of Advanced Microstructures, Nanjing University, Nanjing 210093, P. R. China

[d.] Jiangsu Provincial Key Laboratory for Nanotechnology, Nanjing University, Nanjing 210093, P. R. China

Experimental

Preparation of precursor solutions

Unless stated otherwise, all reagents and materials were purchased commercially from Xi'an Polymer Light Technology Corp. and used as received without further purification. To prepare the PbI_2 precursor solution, PbI_2 of 0.461 g was dissolved in DMF (N, N-Dimethylformamide) of 1 mL and the mixture was stirred at 70 °C until clarification in the N_2-filled glove box. To prepare $CH_3NH_3PbI_3$ perovskite precursor solution, PbI_2 of 0.461 g and CH_3NH_3I of 0.159 g was mixed in DMF of 625 μL and DMSO (Dimethyl sulfoxide) of 76 μL and the mixture was stirred at room temperature until clarification in the N_2-filled glove box. To prepare the hole-transporting-material (HTM) precursor solution, we dissolved spiro-OMeTAD of 0.145 g in chlorobenzene of 2 mL plus 4-tert-butylpyridine of 28 μL and Li-bis-(trifluoromethanesulfonyl)imide of 35 μL which was previously dissolved in acetonitrile with a concentration of 520 mg mL^{-1} successively and then the mixture was stirred at room temperature until clarification in the N_2-filled glove box.

Fabrication of devices

First of all, a compact TiO_2 layer was spin-coated on the pre-cleaned FTO glass via the common routine and then annealed in the air at 480 °C for 2 h. Then the $CH_3NH_3PbI_3$ perovskite precursor solution mentioned above was spin-coated on the prepared substrate with the speed of 4000 rpm for 30 s in the N_2-filled glove box. Afterwards, the $CH_3NH_3PbI_3$ perovskite precursor film was annealed at 110 °C for 15 min and then cooled down to the room temperature in the N_2-filled glove box. And besides, for the PbI_2 heterogeneous cap, the prepared PbI_2 precursor solution mentioned above was spin-coated on the prepared substrate which was pre-heated at 50 °C with the

speed of 3000 rpm for 25 s in the N_2-filled glove box. Then the precursor PbI_2 film was annealed at 110 ^oC for 15 min in the N_2-filled glove box. Specially, during the heterogeneous cap face-to-face annealing process, the $CH_3NH_3PbI_3$ perovskite film was covered with the prepared PbI_2 heterogeneous cap or the substrate which is noted as the TiO_2 heterogeneous cap in our work during thermal annealing. Afterwards, the cap was removed and the $CH_3NH_3PbI_3$ perovskite film was cooled down to the room temperature. Next, the HTM precursor solution was spin-coated on the $CH_3NH_3PbI_3$ perovskite film with the speed of 3000 rpm for 25 s in the N_2-filled glove box. Finally, the Ag back contact electrode with an active area of 0.09 cm^2 was deposited by the vacuum thermal evaporation method.

Characterizations

The XRD patterns were collected on a Rigaku Ultima III X-ray diffractometer using Cu-K_α radiation (λ=0.154178 nm) with the speed of 10^o min^{-1}. An FEI Helios 600i was employed to characterize the surface morphology of the samples. The AFM analysis was performed on an MFP3D 50 microscope (Asylum Research, MFP-3D-SA, USA) with a cantilever operating in the tapping mode. A Shimadzu UV-2550 spectrometer with an integrating sphere was used to investigate the absorption properties of the samples. The PL spectra were conducted at the room temperature on a fluorescence spectrophotometer with the excitation wavelength of 515 nm. The J-V measurements of the fabricated solar cells were carried out in the air with the relative humility below 30% on a Keithley 2400 source measurement unit under AM 1.5 illuminations (standard 100 Mw/cm^2) cast by an Oriel 92251A-1000 sunlight simulator calibrated by the standard reference of a Newport silicon solar cell. The J–V curves of solar cells were recorded by the scans with a voltage step of 10 mV and a delay time of 50 ms under an AM 1.5 G sunlight simulator.

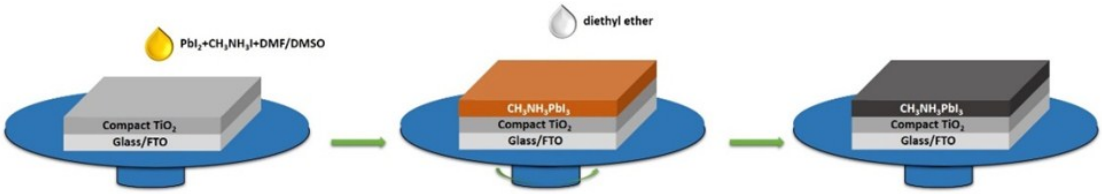

Fig. S1 Diagram of the preparation of the $CH_3NH_3PbI_3$ perovskite film.

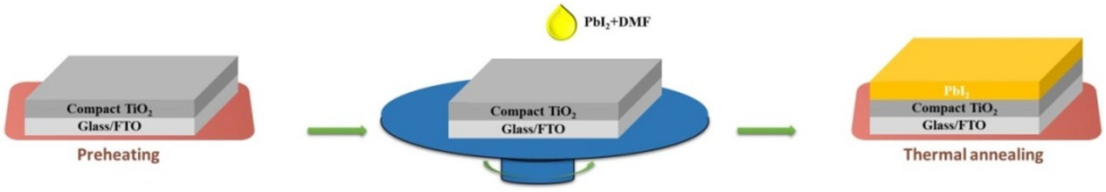

Fig. S2 Diagram of the preparation of the PbI_2 heterogeneous cap.

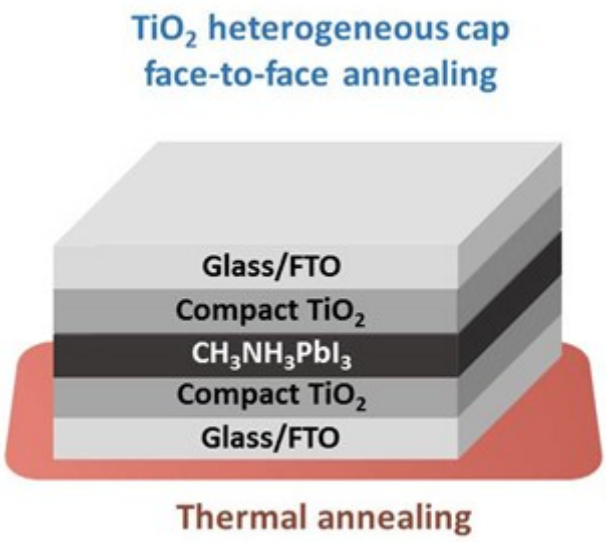

Fig. S3 Diagram of the TiO_2 heterogeneous cap face-to-face annealing process where the $CH_3NH_3PbI_3$ perovskite film is covered face-to-face with a TiO_2 heterogeneous cap during thermal annealing.

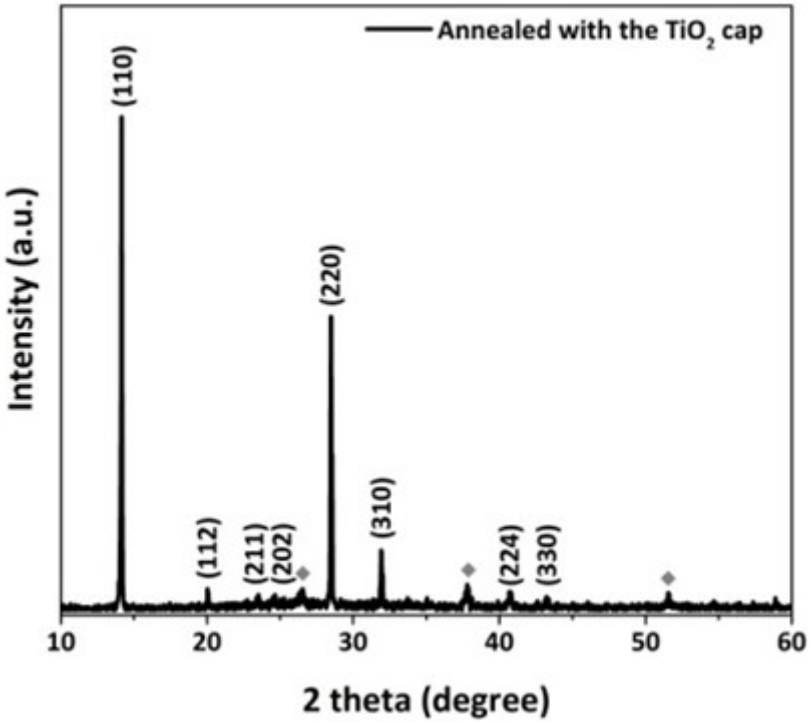

Fig. S4 XRD pattern of the $CH_3NH_3PbI_3$ perovskite film annealed with the TiO_2 cap. The diamond symbols are corresponding to the signals from the TiO_2/FTO substrate.

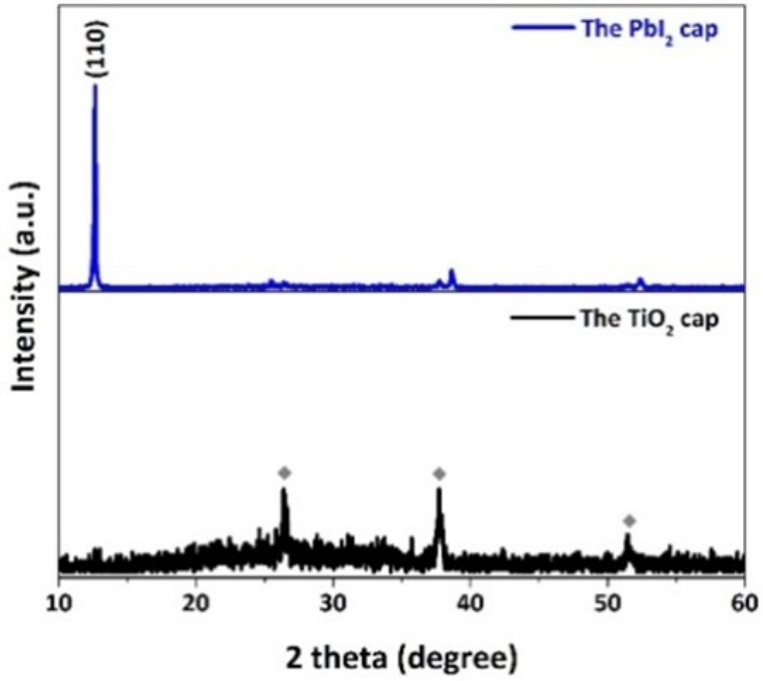

Fig. S5 XRD patterns of the PbI_2 and TiO_2 cap respectively. The diamond symbols are corresponding to the signals from the TiO_2/FTO substrate.

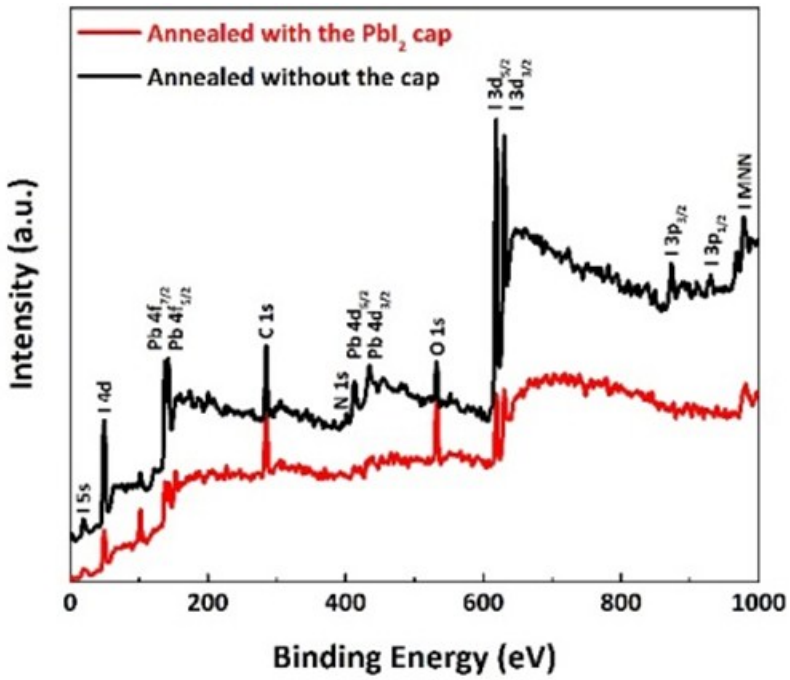

Fig. S6 XPS spectra of the $CH_3NH_3PbI_3$ perovskite films annealed with and without the PbI_2 cap.

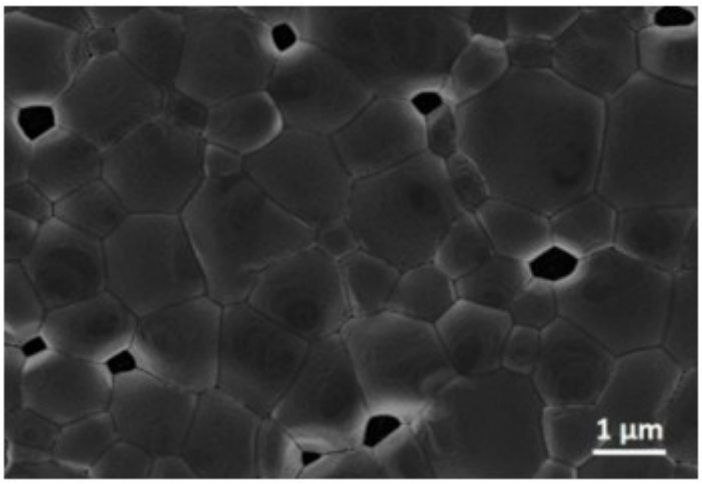

Fig. S7 Top-view SEM image of the $CH_3NH_3PbI_3$ perovskite film annealed with the TiO_2 cap.

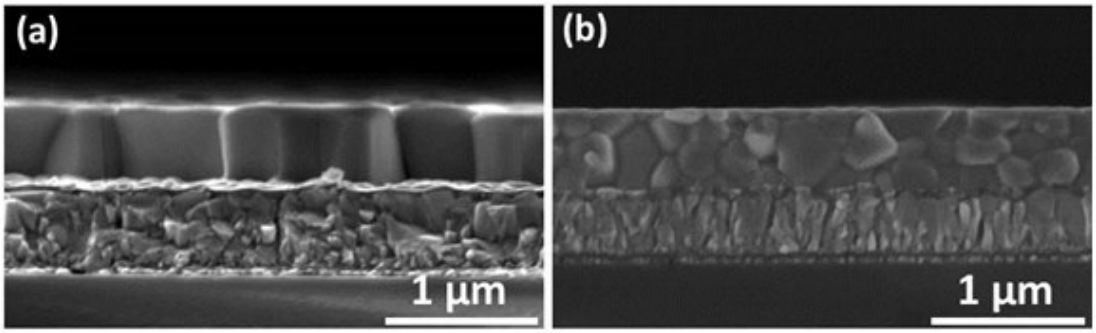

Fig. S8 Cross-sectional SEM images of the $CH_3NH_3PbI_3$ perovskite films annealed with (a) and (b) without the PbI_2 cap.

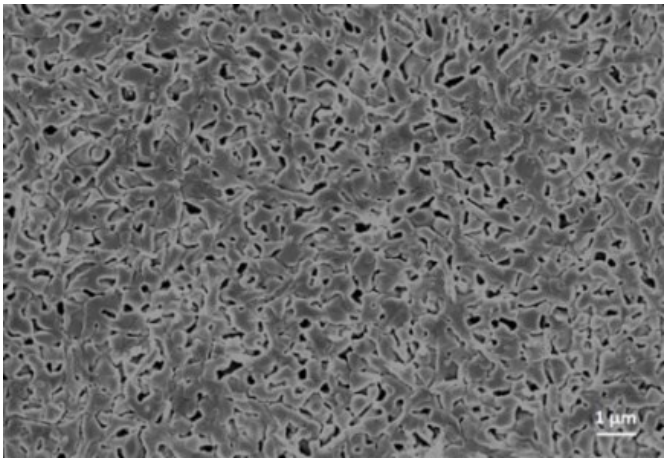

Fig. S9 Top-view SEM image of the PbI_2 cap.

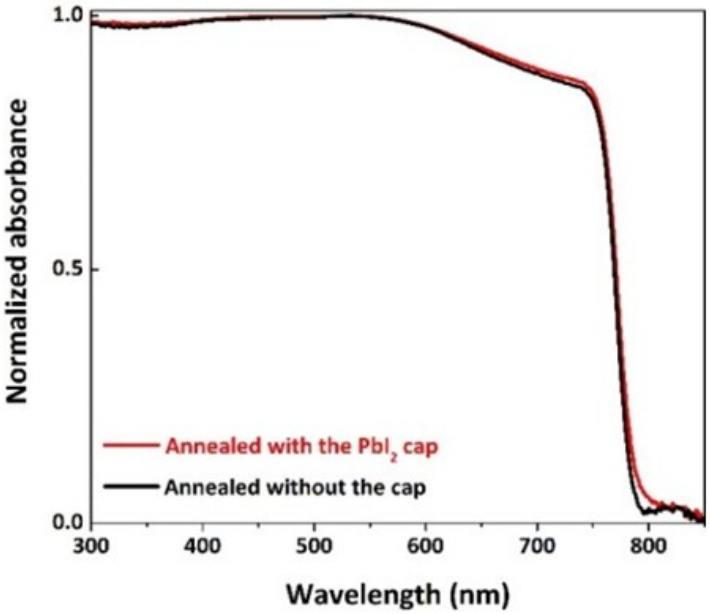

Fig. S10 Normalized UV-Vis spectra of the $CH_3NH_3PbI_3$ perovskite films annealed with and without the PbI_2 cap.

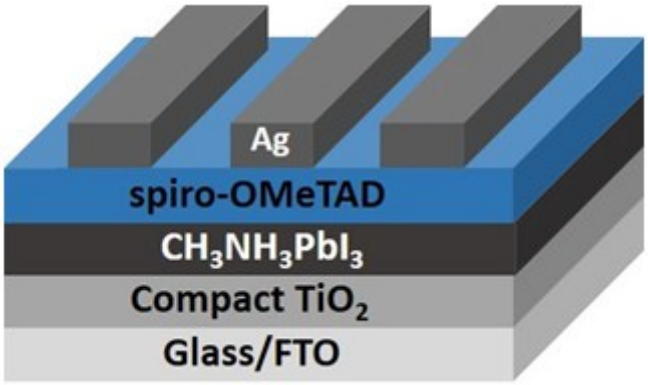

Fig. S11 Schematic of the structure of the fabricated perovskite solar cell.

Table S1 Summary of the PV performance parameters of the fabricated perovskite solar cell with the $CH_3NH_3PbI_3$ perovskite film annealed with the PbI_2 cap, TiO_2 cap, or without cap.

Sample	J_{sc}(mA/cm^2)	V_{oc}(V)	FF	PCE(%)
With PbI_2 cap	23.41	1.07	0.70	17.57
Without cap	22.62	1.05	0.60	14.19
With TiO_2 cap	19.28	0.99	0.66	12.62

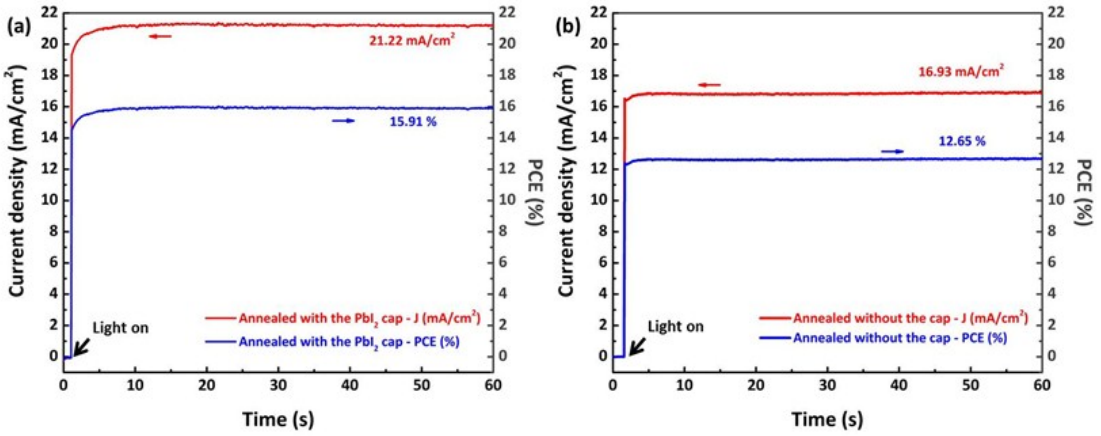

Fig. S12 Stabilized current density and PCE output (measured at 0.75 V) of the fabricated perovskite solar cells annealed with the $CH_3NH_3PbI_3$ perovskite films (a) with and (b) without the PbI_2 cap.

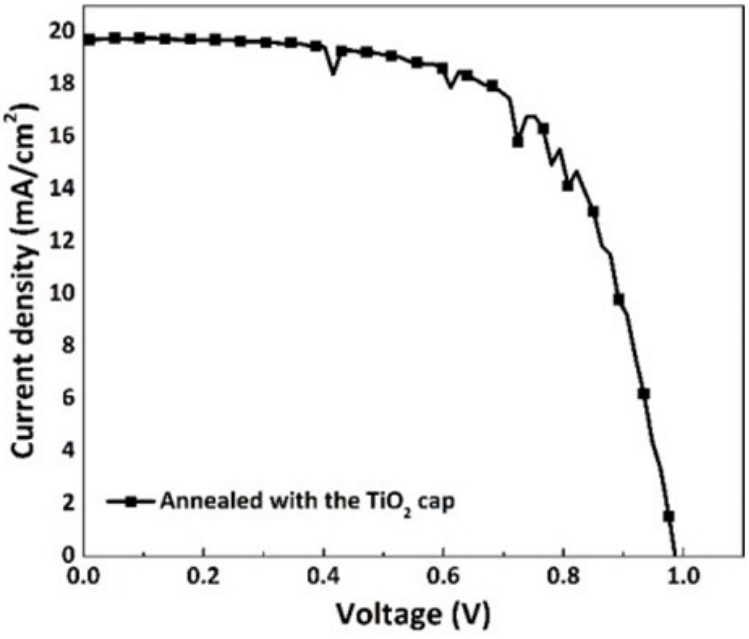

Fig. S13 Optimized J-V curve of the fabricated perovskite solar cell with the $CH_3NH_3PbI_3$ perovskite film annealed with the TiO_2 cap.

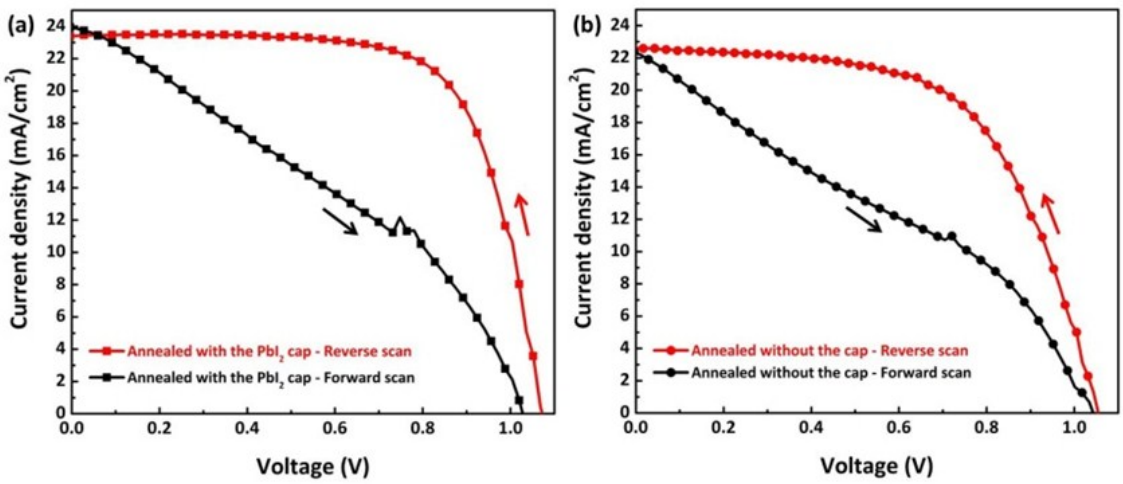

Fig. S14 J-V curves measured at reverse scan (1.2 V to - 0.1 V) and forward scan (-0.1 V - 1.2 V) of the fabricated perovskite solar cell with the $CH_3NH_3PbI_3$ perovskite films annealed (a) with and (b) without the PbI_2 cap.

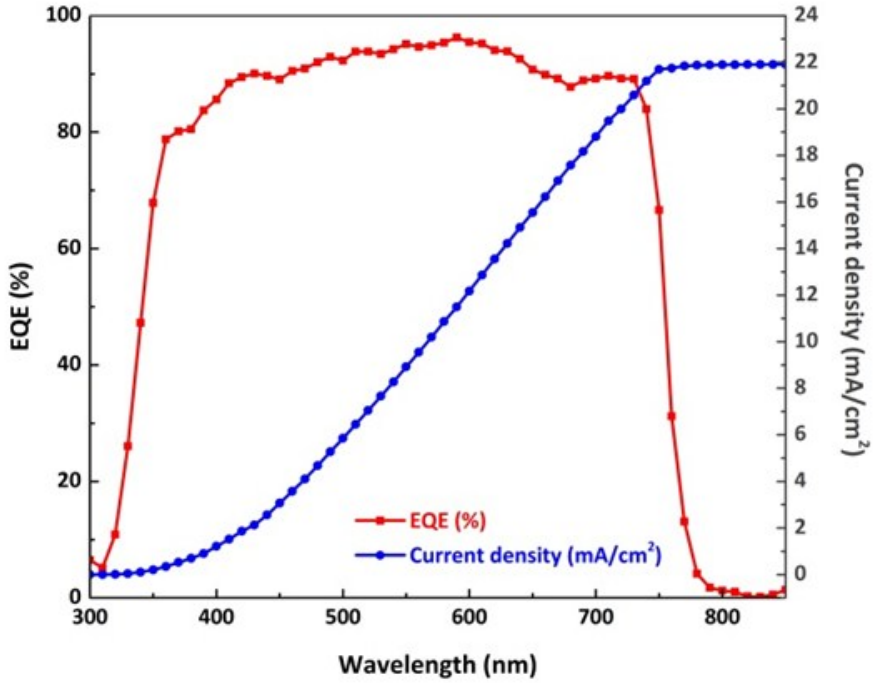

Fig. S15 EQE curve taken with the monochromatic light without applied white-light bias and correspondingly calculated J_{sc} curve of the optimized perovskite solar cell with the $CH_3NH_3PbI_3$ perovskite film annealed with the PbI_2 cap.

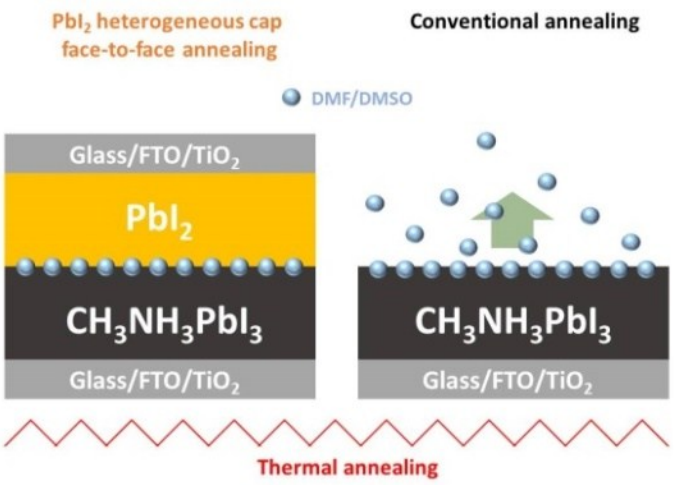

Fig. S16 Diagram of the residual DMF or DMSO solvent molecules at the interface between the PbI_2 heterogeneous cap and the $CH_3NH_3PbI_3$ perovskite film during the PbI_2 heterogeneous cap face-to-face annealing process. The blue balls are sketches of DMF or DMSO solvent molecules.